Understanding food web mercury accumulation through trophic transfer and carbon processing along a river affected by recent run-of-river dams

Dominic E. Ponton[1], Raphaël A. Lavoie[1,2], Maxime Leclerc[1], François Bilodeau[3], Dolors Planas[4], Marc Amyot[1*]

[1] Groupe de recherche interuniversitaire en limnologie (GRIL), Département des sciences biologiques, Université de Montréal, Montréal, Québec, Canada, H2V 0B3.

[2] Canadian Wildlife Service, Environment and Climate Change Canada, 801-1550 avenue d'Estimauville, Québec, Québec, Canada, G1J 0C3.

[3] Hydro-Québec, Direction Environnement, 800 boul. De Maisonneuve Est, Montréal, Québec, H2Z 1A4.

[4] GRIL, Département des sciences biologiques, Université du Québec à Montréal, Montréal, Québec, Canada, H2X 3Y7.

Word count : 5325 (without abstract and references) + 1800 (6 figures at 300 words) = 7125.

*Corresponding author: m.amyot@umontreal.ca

Keywords: mercury, carbon, nitrogen, trophic magnification slope, run-of-river, food web

ABSTRACT

Unlike large dams which favor methylation of Hg in flooded soils over long periods, run-of-river dams are designed to flood a limited area of soils and are therefore not expected to significantly affect mercury (Hg) cycling or carbon processing. We studied the Hg and carbon cycles within food webs from several sectors along the Saint-Maurice River, Quebec, Canada, that differ in how they are influenced by two run-of-river dams and other watershed disturbances. We observed peak Hg concentrations in fish five-year post-impoundment, but these levels were reduced three years after this peak. Methylmercury concentrations in low trophic level fish and invertebrates were related to their carbon source ($\delta^{13}C$) rather than their trophic positions ($\delta^{15}N$). Biomagnification, measured by trophic magnification slopes, was driven mainly by methylmercury concentrations in low trophic level organisms and environmental factors related to organic matter degradation and Hg methylation. River sectors, $\delta^{13}C$, and $\delta^{15}N$ predicted up to 80% of the variability in food web methylmercury concentrations. The installation of run-of-river dams and the related pondages, in association with other watershed disturbances, altered carbon processing, promoted Hg methylation and its accumulation at the base of the food web, and led to a temporary increase in Hg levels in fish.

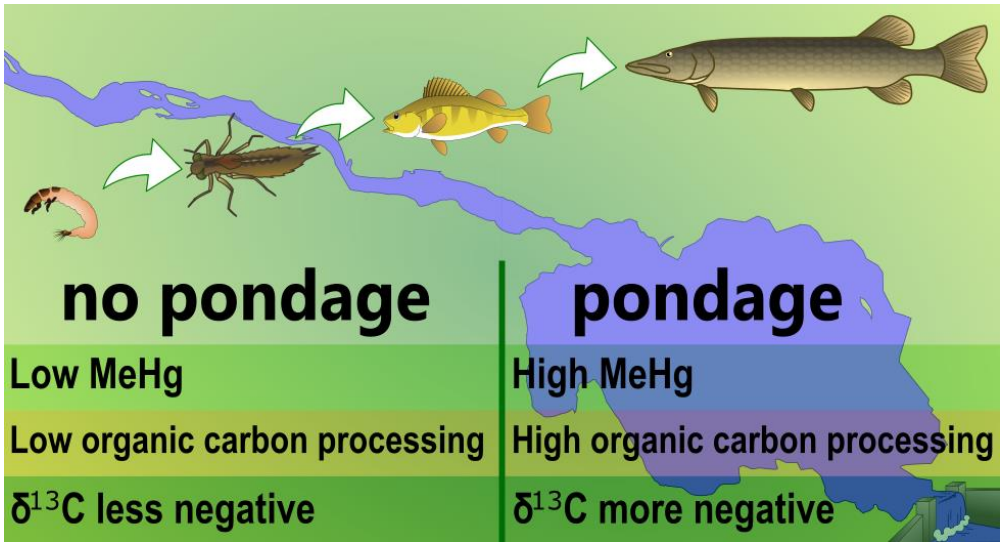

TOC Art; Ponton et al., 2021

INTRODUCTION

Worldwide, rivers are increasingly fragmented by dams built to provide services such as irrigation, drinking water, and hydroelectricity.[1] Hydroelectricity represents approximately 16% of the world's electricity production;[2] however, as countries attempt to reduce their carbon emissions, it is anticipated that there will be an expansion of hydroelectric power plants, tripling river fragmentation in the next decades.[2, 3] In addition to altering river dynamics and carbon fluxes,[4, 5] the installation of hydroelectric dams often causes extensive upstream flooding, which can lead to the transient contamination of food webs by mercury (Hg) and methylmercury (MeHg) released by the flooded soils. MeHg in top predatory fish may reach levels that surpass consumption recommendations issued by health agencies (0.5 μg Hg/g wet weight).[6, 7] Run-of-river hydroelectric power plants are generally considered to have fewer environmental impacts than power plants associated with large-scale reservoirs[7-9] because run-of-river dams require only limited water storage (called pondage) or even no storage at all.[3] Nevertheless, studies of the potential role of run-of-river power plants on Hg food web dynamics and the related consequences of alterations of the Hg and carbon cycles remain scarce.

Run-of-river impoundments could favor Hg methylation because flooded soils serve as a substrate for redox conditions conducive to Hg methylation by organic matter–degrading microorganisms.[10] Microbial activity linked to organic matter degradation can alter carbon cycling by releasing carbon dioxide (CO_2), methane (CH_4), and transformed organic matter into the overlying water.[11-13] To better understand changes in MeHg concentrations ([MeHg]) in aquatic wildlife following impoundment, the link between carbon processing and Hg methylation must

64 therefore be assessed. The evaluation of these links in aquatic ecosystems can rely on tracing of
65 isotopic signature of carbon ($\delta^{13}C$) in different matrices.[14]
66
67 River carbon and Hg cycles are also influenced by anthropogenic and natural disturbances in the
68 surrounding watershed.[15] For instance, logging and wildfires can lead to the leaching of Hg,
69 organic matter, and nutrients into a river system, thereby affecting Hg concentrations in food
70 webs.[16] The construction of run-of-river facilities could exacerbate this phenomenon through the
71 creation of permanent floodplains and sedimentation zones upstream of the dam, with yet
72 unexplored effects on Hg cycling.[4]
73
74 Once Hg has been microbially methylated, it biomagnifies efficiently.[17] MeHg trophic transfer
75 efficiency is often evaluated through the use of the trophic magnification slope (TMS), which is
76 the slope of the regression between log-transformed [MeHg] in organisms and their nitrogen
77 isotopic signature ($\delta^{15}N$).[18] The TMS can vary due to changing environmental factors, including
78 nutrient concentrations;[19] however, more studies are needed to understand the factors
79 influencing TMS. No study has used TMS to trace spatial changes in Hg dynamics along run-of-
80 river systems but fragmentation of rivers by run-of-river dams may affect invertebrate and fish
81 community structure, thereby modifying Hg food web dynamics.[20-22]
82
83 This study focuses on a medium-size river system affected by the construction of a pair of run-of-
84 river power plants and characterized by a surrounding watershed that has been recently
85 disturbed by constructed wetlands, forest fires and logging. Our main objective was to study the

consequences of run-of-river pondages and concomitant landscape disturbances on carbon processing and Hg trophic transfer within the aquatic food web. More specifically, we investigated (1) how fish Hg concentrations fluctuated in relation to disturbances over time; (2) how Hg methylation and accumulation in the food web was linked to proxies of carbon processing; and (3) how biomagnification varied as a function of environmental disturbance along the river. This study provides one of the first investigations of the link between carbon and Hg cycles in a river impacted by run-of river dams.

METHODS

Study Area. The Saint-Maurice River, central Quebec, Canada, is 563 km long and has an average annual flow of 730 m^3/s at the river mouth. The river runs mainly from the Gouin Reservoir that was flooded in 1918. Fish Hg concentrations in this reservoir have since returned to pre-impoundment levels.[7, 23] Chute-Allard (CA) and Rapides-des-Coeurs (RDC) are two consecutive run-of-river power plants, located 30 km apart along the Saint-Maurice River. Both were built in 2008 close to the Wemotaci First Nation Reserve (47°54.140'N, 73°47.212'W), in which resides an Atikamekw community (Figure 1). The emplacement of these two dams led to 2 and 3.7 km^2 impoundments of forested land for the CA and RDC power plants, respectively. Figure 1 illustrates the flooded areas (in dark blue) present in the CA pondage. Wetlands were created by digging numerous channels (0.1 km^2; CC) upstream of CA pondage to compensate for habitat modification and increase biodiversity. Two years post-impoundment, a wildfire (200 km^2) occurred near the CA power plant and related pondage. Logging has also been extensive around the RDC sector (see Figure 1 for logged and burned areas). Logs were floated on the river until

the mid-1990s. The Rapide-Blanc dam was constructed in 1930 and formed the 82 km^2 Blanc Reservoir (Figure 1) immediately downstream of the RDC power plant. Water levels in this reservoir fluctuate markedly (9 m drawdown), and this water body is intensively used by anglers. These perturbations (constructed wetlands, wildfire, logging, various forms of river dam) provided a unique opportunity to study the impact of multiple disturbances on the carbon and Hg cycles of the river. Figure 1 illustrates the nine studied sectors. Ordered from upstream to downstream, they are a control sector downstream of the Gouin Reservoir (REF1), the Chaudière Rapids (CR), the confluence of the Najoua and Saint-Maurice rivers (NSM), the second upstream reference sector (REF2), the confluence of the Manouane and Ruban rivers (MR), the constructed wetland channels (CC), the upstream pondage of the Chute-Allard power plant (CAUP), downstream of the Chute-Allard power plant (CADW), the Rapides-des-Coeurs pondage (RDC), and the Blanc Reservoir (BR). The sectors CC, CAUP, RDC, and BR are considered as flooded sectors. Water retention times are as follows in pondages and reservoir: CAUP: 15 h, RDC: 51 h, and BR: 14 days.

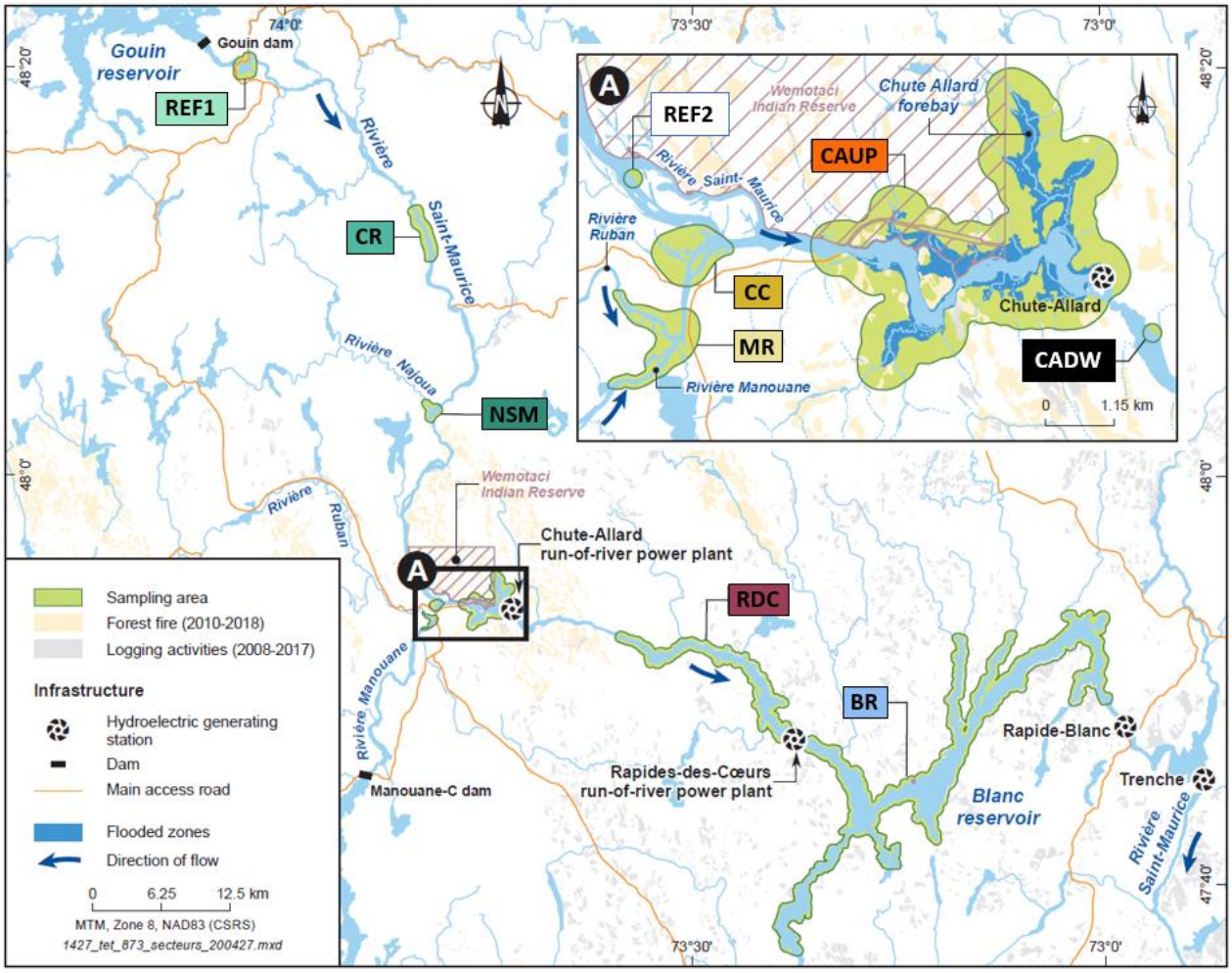

Figure 1. Sampled sectors along the Saint-Maurice River (Haute-Mauricie region, Quebec, Canada) from upstream (upper left) to downstream (lower right). The sampled sectors are downstream of the Gouin Reservoir (REF1), the Chaudière Rapids (CR), the confluence of the Najoua and Saint-Maurice rivers (NSM). In the inset map (A), the sectors are the second reference sector (REF2), the confluence of the Manouane and Ruban rivers (MR), the constructed wetland channels (CC), the pondage upstream of the Chute-Allard power plant (CAUP), and the sector downstream of the Chute-Allard power plant (CADW). The two most downstream sectors are the pondage upstream of the Rapides-des-Coeurs power plant (RDC) and the Blanc Reservoir (BR).

Fish Sampling. In August 2013 and 2016 (5 and 8 years post-impoundment), a private consulting firm (AECOM, Trois-Rivières, QC, Canada) collected 584 and 1404 fish, respectively. These fish were used for community[24, 25] and muscle [Hg] surveys.[26, 27] The collected species were yellow perch (*Perca flavescens*), walleye (*Sander vitreus*), northern pike (*Esox Lucius*), longnose sucker (*Catotomus catostomus*), white sucker (*Catotomus commersonii*), lake whitefish (*Coregonus*

137 *clupeaformis*), and fallfish (*Semotilus corporalis*). Fish weight and length were measured, and
138 muscle samples were collected close to the dorsal fin. To compare natural and post-
139 impoundment [Hg] ranges, we also used samples of northern pike (*n* = 204), walleye (*n* = 259),
140 and yellow perch (*n* = 38) collected between 1990 and 1992 from 3 to 4 unimpacted lakes
141 (according to species) from the Haute-Mauricie region and from 5 to 6 sectors along the Saint-
142 Maurice River. Those sites are referred to as control sectors (CTL) and details are given in
143 Supplementary Information (SI, Text S1 and Table S1).
144
145 From the fish collected in 2013 and 2016, we selected 354 and 842 specimens, respectively, for
146 total Hg (THg) analysis. Our aim was to analyze 30 individuals/species/site.[26, 27] From the 842
147 specimens analyzed for THg in 2016, we selected 332 fish samples for MeHg analysis. Those were
148 selected at random and in duplicates for six size classes per species. Therefore, where possible,
149 we had 12 samples per species per sector available for [MeHg], $\delta^{13}C$, and $\delta^{15}N$ analyses. Juvenile
150 fallfish (hereafter called minnows) were also collected in 2018 with a hand net from the side of a
151 boat.[28]
152
153 **Invertebrate Sampling.** We collected littoral invertebrates using a kick-net from several micro-
154 niches including rocks, sediments, and macrophytes. We sampled zooplankton from shallow bays
155 using a plankton net. In our survey, we collected invertebrates from 23 families (SI, Text S2). For
156 determining the $\delta^{15}N$ baseline in a given sector, we considered zooplankton and the following
157 invertebrate families as the primary consumers: Asellidae, Beatiscidae, Gammaridae,

158 Hydrobiidae, Limnephilidae, Lymnaeidae, Phryganeidae, Physidae, Planorbidae and Sphaeriidae
159 (SI, Table S2).
160
161 **Hg Analysis.** Total Hg was measured in dried muscle tissues using a direct Hg analyzer (DMA-80,
162 Milestone) at University of Montreal and by an external certified laboratory (Veritas Laboratories,
163 Montreal, QC; ISO 17025) using atomic absorption spectrometry. DMA-80 analyses included
164 measurements of the reference material TORT-2 (National Research Council of Canada) every ten
165 samples. The measured [THg] in TORT-2 was 315 ± 5 (± confidence interval (CI), n = 12), a value
166 within the certified range (270 ± 60 ng/g dw, ± CI). Veritas performed three analytical replicates
167 on 45 fish samples, and the coefficient of variation was on average 5%. Both methods gave very
168 similar results during an intercalibration exercise ($[THg]_{DMA} = 1.01 \pm 0.01 * [THg]_{Veritas} + 0.03 \pm 0.01$
169 µg/g ww, ± standard error (SE), r^2 = 0.99, n = 103; SI, Text S3).
170
171 For MeHg analysis in fish tissue, we digested 8 to 10 mg of dry tissue in 10 mL diluted HNO_3 (4 M)
172 overnight at 65 °C.[29] A 25 or 50 µL aliquot was added to 30 mL of Milli-Q water buffered with
173 acetate. We added tetraethylborate for ethylation, and we detected MeHg through cold vapor
174 atomic fluorescence spectrometry (Tekran Series 2700, Tekran Instruments Corporation)
175 according to the U.S. EPA method 1630 (detection limits (DL) of 0.01 ng/L or 0.1 ng/g dw). The
176 reference material TORT-2 was digested with the samples for each analytical day. The average
177 value was 151 ± 2 ng/g dw (± CI; n = 57), and the certified value was 152 ± 13 ng/g (± CI). We
178 modified our analytical protocol slightly to measure THg and MeHg from the same tissue digestate

when the available biomass was limited. This procedure was tested in our laboratory and is described in the SI (Text S3).[30]

Nitrogen and Carbon Isotope Analyses. Fish and invertebrate samples were freeze-dried in acid-washed glass jars. Samples were homogenized with a glass pestle and weighed (1.0 ± 0.2 mg) in tin cups. A similar preparation was applied to the reference materials. We analyzed samples with a Micromass Isoprime 100 isotope ratio mass spectrometer coupled to an Elementar Vario MicroCube elemental analyzer in continuous flow mode at the GEOTOP laboratory (UQAM, Montreal, QC, Canada). Our results are given in delta units (δ) in per mill (‰) vs air ($\delta^{15}N$) for nitrogen and Vienna Pee Dee Belemnite ($\delta^{13}C$) for carbon isotopes. The overall analytical uncertainty is better than ±0.2‰ and ±0.1‰ for nitrogen and carbon, respectively (SI, Text S4).

Water Sampling and Analyses. We collected the river water samples from littoral sites at 1 m depth using Teflon tubing attached to a peristaltic pump. Water samples were collected as triplicates using either no filtration or an in-line Whatman 0.45 µm filtration capsule attached to the tubing. All manipulations were made following trace metal protocols. Details regarding the analysis of aqueous Hg, dissolved organic carbon (DOC), gas, and nutrients are given in SI (Text S5).

Data Analyses and Statistics. From the [THg] of 30 individuals from a given fish species, we used polynomial regressions of total [Hg] as a function of fish length to obtain standardized [THg] for a given length ($[THg_{std}]$, northern pike: 600 mm, walleye: 400 mm, and yellow perch: 160 mm)

following Tremblay et al.[31] To calculate the control sector [THg_{std}], we used all fish samples of a given species from all control sectors to produce a single polynomial regression.

Given the heterogeneity among the sectors, we adjusted the $\delta^{15}N$ of all organisms according to a $\delta^{15}N$ baseline. The $\delta^{15}N$ baseline for each sector (*j*) was determined as the average $\delta^{15}N$ of primary consumers ($\delta^{15}N_{Baseline\,j}$; SI, Table S2). The $\delta^{15}N_{Baseline\,j}$ was subtracted from the $\delta^{15}N$ value of each organism (*i*) in each sector (*j*) to obtain adjusted $\delta^{15}N_{ij}$ ($\delta^{15}N_{adj}$) values for all organisms according to the equation:

$$\delta^{15}\mathrm{N}_{\mathrm{adj}} = \delta^{15}\mathrm{N}_{ij} - \delta^{15}\mathrm{N}_{\mathrm{Baseline}\,j} \quad (1)$$

Assuming an increase in $\delta^{15}N$ values of 3.8‰ per trophic level, $\delta^{15}N_{adj}$ values for fish ranged from 1.7‰ to 9.3‰, covering about two trophic levels.[32] To interpret our results, we separated the collected fish into two groups, i.e., low trophic level fish having $\delta^{15}N_{adj}$ <5 (trophic level <3.5) and the remaining fish considered as high trophic level fish ($\delta^{15}N_{adj}$ >5; trophic level >3.5). We selected the value $\delta^{15}N_{adj}$ = 5 on the basis of the inflection point in the data (Figure S3). We considered that this inflection corresponds to a shift in the diet between the two fish groups. Furthermore, we selected this value to include most juvenile fallfish and suckers, given their diet, in the low trophic level fish category.

The [Hg] and [MeHg] were log-transformed to meet the conditions of normality. To test the link between [MeHg] and the $\delta^{13}C$ and $\delta^{15}N_{adj}$, we performed simple regressions when conditions were respected. To test whether trophic magnification slopes differed among sectors, we

performed analyses of covariance (ANCOVA) followed by post hoc Tukey test (all sectors paired, *lsmeans* R package, $\alpha = 0.05$).

Linear mixed effect models (R package *lmer*) were conducted to explain variations in organismal [MeHg] (response variable) with $\delta^{15}N_{adj}$, $\delta^{13}C$, or $\delta^{15}N_{adj}*\delta^{13}C$ (predictor variables, fixed effects), and river sectors set as a random effect. We compared those three models ($\delta^{15}N_{adj}$, $\delta^{13}C$, or $\delta^{15}N_{adj}$ + $\delta^{13}C$) among different groups, i.e. primary consumers, secondary consumers, all invertebrates, low trophic level fish, high trophic level fish, all fish, and all organisms. We selected the most parsimonious model by relying on the Akaike information criterion (an AIC >4 between the best pair of models; Table S3).[33] Residuals of the best model were evaluated for normality and homoscedasticity. R (version 3.5.3), RStudio (version 1.3.1056), and Sigmaplot 13 (Systat Software Inc.) software were used for all our statistical analyses and their visualization.

RESULTS AND DISCUSSION

Fast Rise and Decline of Fish Hg Concentrations in Run-of-River Pondages. For both run-of-river pondages, CAUP and RDC, the [THg_{std}] in northern pike, walleye, and yellow perch rose 2.1 ± 0.6 (± standard deviation (SD)) times in 2013, five years after impoundment, compared with measured [THg_{std}] from the control sectors (CTL; Figure 2). For the older reservoir downstream (BR), the [THg_{std}] increase was only 1.4 ± 0.2 times higher. Walleye and yellow perch [THg_{std}] were 1.8 ± 0.1 times higher in CAUP and RDC in 2013 relative to the control sectors (Figure 2a, b). In contrast, the increase in northern pike [THg_{std}] was more pronounced five years post-impoundment with [THg_{std}] 2.8 ± 0.2 times higher than the control sectors (Figure 2c). Elevated

fish [Hg] led regional health agencies to establish more stringent guidelines in regard to fish consumption by the surrounding communities.[24] In 2013, the [THg_{std}] for northern pike and walleye in the run-of-river pondages were approx. 2.0 and 1.2 µg/g ww, respectively, levels above the Health Canada recommendations for commercially sold fish (0.5 µg/g ww).[6]

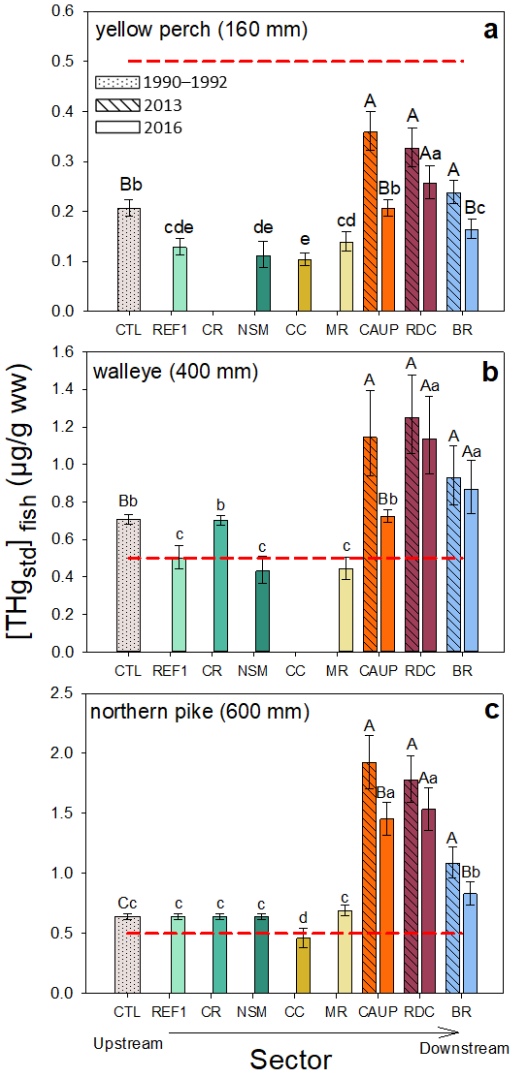

Figure 2. Length-standardized total Hg concentrations ([THg_{std}] µg/g wet weight (ww) ± CI) five (2013) and eight years (2016) after CAUP and RDC impoundments for (a) 160 mm yellow perch, (b) 400 mm walleye, and (c) 600 mm northern pike from sampled sectors on the Saint-Maurice River (Quebec, Canada). Sectors are presented from upstream to downstream (Figure 1), with the exception of the regional control sectors (CTL, see Methods and Text S1). CTL, REF1, CR, and NSM are upstream unimpacted sectors, CC is the constructed wetland, CAUP and RDC are the run-of-river pondages, and BR is the downstream reservoir. Significant differences (p <0.05) between years (capital letters) and sectors (2016, lowercase letters) are presented. The red dashed line is the standard Health Canada limit for fish commercialization.

To assess the spatial variability of fish Hg contamination, we sampled a greater number of sectors in 2016 than in 2013 (Figure 2). The additional 2016 sectors produced [THg_{std}] similar or below the ones from control sites (Figure 2). We observed an overall decline in [THg_{std}] in both pondages and BR between 2013 and 2016. Average fish [THg_{std}] from 2016 was 70% ± 20% the 2013 average [THg_{std}] in CAUP, RDC, and BR, although this decrease was not significant in RDC. [THg_{std}] decreases in walleye and yellow perch were important in CAUP and BR and reached the standardized concentration of control sites, whereas northern pike [THg_{std}] remained above this concentration. A follow-up study is required to determine whether Hg concentrations will continue to decrease in northern pike and fish within the RDC pondage to reach the concentrations found in the control sites. In the large reservoirs from northern Quebec, the maximum [Hg] in fish predators are recorded typically 9–14 years post-impoundment. These concentrations then gradually decrease to natural background values approx. 30 years post-impoundment.[7] In comparison, our studied run-of-river systems present a faster Hg dynamics, which is to be expected given the more limited water retention time (CAUP: 15 h, RDC: 51 h) and the relatively small flooded area (CAUP: 2 km^2, RDC: 3.7 km^2).

The only published studies on Hg bioaccumulation in run-of-river pondages found no significant differences in the Hg accumulation in macroinvertebrates, fish and birds between run-of-river pondages and non-impounded rivers.[9, 34] In contrast, in large reservoirs such as those downstream of the La Grande River complex (QC, Canada; 740–2630 km^2 of flooded land), northern pike [THg_{std}] (700 mm) were 2.1 ± 0.6 µg/g ww five years after impoundment, thus

similar to those measured in northern pike (600 mm) from CAUP and RDC in 2013 (Figure 2c). Walleye [THg_{std}] (400 mm) was two times lower in CAUP and RDC (2013; Figure 2b) compared with walleye from the large northern Quebec reservoirs, five years after impoundment (2.3 ± 0.6 µg/g ww).[7] Higher Hg accumulation in northern pike than walleye in our systems may suggest that pike feeds in the shallower flooded zones characterized by a higher MeHg exposure, in contrast with walleye living in deeper waters where upstream uncontaminated water flow is greater.[35] These comparisons suggest a marked increase in fish [Hg] from CAUP and RDC pondages considering their small impoundment surface (CAUP: 2 km^2; RDC: 3.7 km^2) and water residence time (CAUP: 15 h; RDC: 51 h)[9, 34] More studies are needed to evaluate if this case is an exception or representative of boreal run-of-river systems.

We tested several hypotheses that could have explained this fish Hg rise. First, we observed a marked increase in yellow perch abundance in the CAUP and RDC sectors relative to pre-impoundment conditions (Figure S1). This increase could have led to cannibalism and an increased food chain length and Hg trophic transfer; however, a detailed analysis revealed that this demographic shift did not change sector specific trophic length and yellow perch $\delta^{15}N_{adj}$. Furthermore, yellow perch from CAUP and RDC were mostly feeding on invertebrates and not on fish. Thus, Hg accumulation in fish from pondages did not seem related to this demographic change in the yellow perch population (SI, Text S6).

Contrary to our prediction, yellow perch and northern pike from constructed wetland channels (CC) had the lowest [THg_{std}], at levels below those of the control sites (Figure 2). The size

distribution of northern pike and yellow perch in CC vs other sites could not explain these low [THg_{std}] values (SI, Text S6). In contrast, minnows had a slightly higher [MeHg] in CC than in non-impounded sectors (p = 0.06; Figure S2) and invertebrates [MeHg] were among the highest (Table S2 and Figure S8). This sector was highly productive and many factors could have favored Hg methylation in this site.[36] Indeed, we measured high total phosphorous and nitrogen concentrations, and high proportions of MeHg in water (Figure S8). High prey density available for yellow perch could have caused a high fish growth rate and Hg somatic growth dilution leading to low yellow perch and northern pike [Hg_{std}].[37] In a follow-up study, we will investigate how fish growth could influence Hg concentrations using a biodynamic model.[38]

Factors other than impoundment can contribute to the observed marked increase in fish [Hg] in the CAUP and RDC pondages. The severe wildfire that occurred in 2010 (two years after impoundment, Figure 1) may have led to important nutrient and organic matter fluxes into the CAUP pondage.[39] Logging activities around the RDC sector (Figure 1) also likely transferred organic matter to the aquatic system.[40] Logging and wildfires, although the latter to a lesser extent, can increase the [Hg] in stream invertebrates,[41] lacustrine zooplankton, and northern pike.[16, 39] Indeed, Garcia and Carignan[16, 39, 42] observed a moderate rise in organismal MeHg concentrations in lakes impacted by wildfires in contrast to those impacted by logging activities. Similarly, we observed a shorter duration of the [THg_{std}] rise in the sector CAUP, impacted by the 2010 wildfire, in contrast with RDC where the [THg_{std}] in fish did not significantly decrease in 2016 compared to

2013. An ongoing parallel study is attempting to better understand the impact of these landscape perturbations on Hg methylation in the sediments of this system.[43]

Carbon Processing and Hg Methylation. When considering only fish samples, the relationship between [MeHg] and $\delta^{15}N_{adj}$ was not linear but rather presented a V-shape (Figure S3). Low trophic level fish (LTLF) had higher than the expected [MeHg] based on their trophic status; therefore, we tested the [MeHg] and $\delta^{15}N_{adj}$ relationship for these fish. This regression yielded an unusual negative relationship, where $\delta^{15}N_{adj}$ explained only 2% (r^2 = 0.02, p = 0.03, Figure S4a, $AIC_{LTLF\text{-}15N}$ = 23) of the [MeHg] variability. In contrast, the regression of [MeHg] as a function of $\delta^{13}C$ with the same fish was highly significant, and it explained 17% of [MeHg] variability (r^2 = 0.17, p < 0.0001, $AIC_{LTLF\text{-}13C}$ = -5, Figure 3a). A similar trend was found for primary and secondary consumer invertebrates, where [MeHg] variability was, in those two cases, explained better by $\delta^{13}C$ than by $\delta^{15}N_{adj}$ (Figures 3b and 3c, Table S3). These results suggest that organisms with more negative $\delta^{13}C$ values have a higher MeHg exposure than organisms with less negative $\delta^{13}C$ values. Furthermore, the $\delta^{13}C$ for high trophic level fish was significantly lower in the flooded sectors (CC, CAUP, RDC, BR) than in the upstream sites (Figure S5). This analysis of variance was performed using either all fish combined (Figure S5a) or either only northern pike or walleye (Figure S5b and S5c, respectively). Carbon processing in the flooded zones appears to have led to depleted $\delta^{13}C$ values and an overall higher MeHg accumulation in food webs. We explored whether water samples could help clarify these biogenic $\delta^{13}C$ patterns.

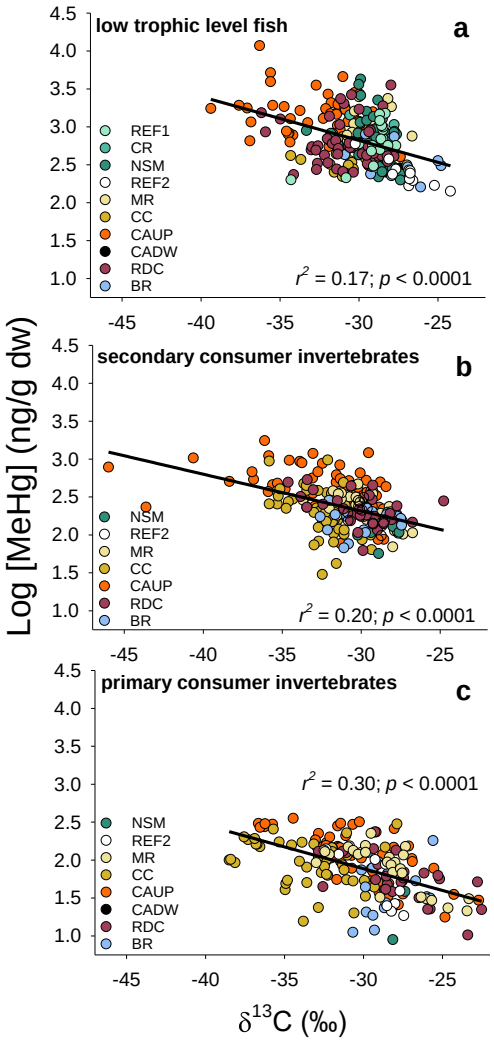

Figure 3. Log-transformed methylmercury concentrations (Log [MeHg], ng/g dw) in (a) low trophic level fish (Low TL), (b) secondary consumer invertebrates, and (c) primary consumer invertebrates as a function of their carbon stable isotopic signature ($\delta^{13}C$, ‰). Organisms were sampled from the Saint-Maurice River, Quebec, at various sectors (see the legend and Figure 1). No invertebrates were collected in sectors REF1 and CR. Flooded sectors are CC, CAUP, RDC, and BR.

Dissolved CO_2 concentrations were negatively correlated with the $\delta^{13}C$ of dissolved CO_2 ($\delta^{13}C$-CO_2; Figure 4a). This highly significant regression (r^2 = 0.86, p < 0.0001) suggests that higher bacterial respiration from the degradation of allochthonous (submerged soils and plants) and autochthonous (periphyton and macrophytes) organic material led to a release of ^{13}C-depleted

354 CO_2.[44, 45] Lennon et al.[44] studied lake systems presenting a gradient in terrestrial organic matter
355 input and suggested that algal uptake of ^{13}C-depleted CO_2 from the bacterial degradation of
356 organic matter led to the large range of measured biogenic $\delta^{13}C$ and $\delta^{13}C$-CO_2, as we observed in
357 our study (Figures 3 and 4).[44, 45] The DOC and TP concentrations were also negatively correlated
358 with $\delta^{13}C$-CO_2 (Figure 4b, c) which suggests that bacterial respiration was directly or indirectly
359 stimulated by the presence of DOC and phosphorous.[46] Furthermore, the proportion of dissolved
360 MeHg in water ($[MeHg]_D/[THg]_D \times 100$) was negatively correlated to the $\delta^{13}C$-CO_2 (Figure 4d).
361 These regressions are indicative of a link between spatial changes of microbial organic carbon
362 processing, nutrient release, and microbial Hg methylation.

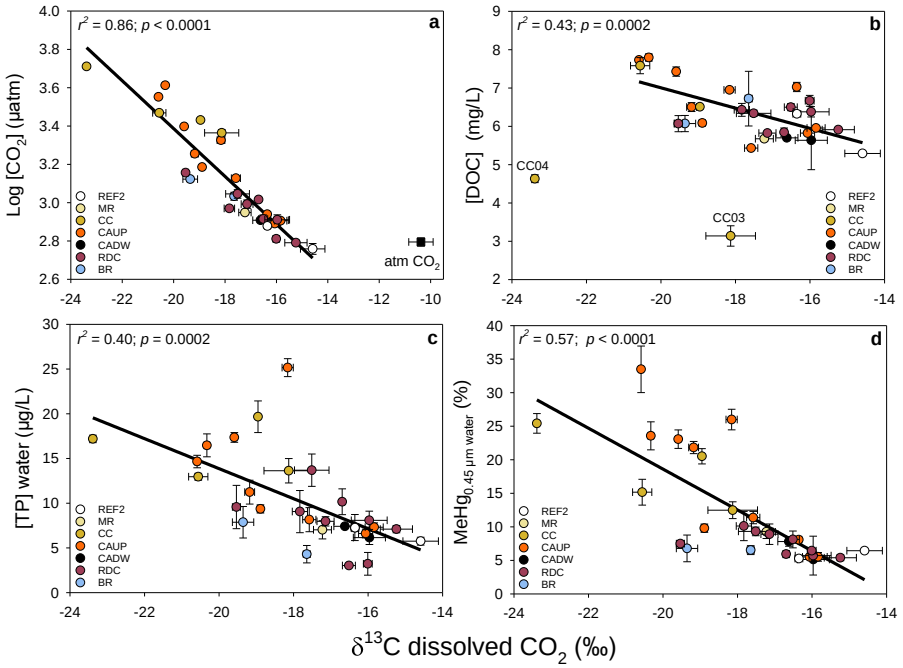

363

364 **Figure 4.** Relationship between the carbon isotopic signature of dissolved carbon dioxide ($\delta^{13}C$-
365 CO_2, ‰) and (a) log-transformed dissolved carbon dioxide concentrations (Log [CO_2], µatm); (b)
366 dissolved organic carbon concentrations ([DOC], mg/L); (c) total phosphorous concentrations
367 ($[TP]_{water}$, µg/L); and (d) the proportions of dissolved methylmercury ($MeHg_{0.45\ µm\ water}$, %,
368 $[MeHg]_D/[THg]_D \times 100$). Standard deviation is presented for all averages (n = 3). The average and
369 SD of atmospheric CO_2 (n = 9) collected over the water surface (close square) is presented in (a).
370 This atmospheric value and identified sites (b: CC03, CC04) were not included in the regression
371 analysis.

The measured DOC (3−8 mg/L) and TP concentrations (3−25 µg/L) are in the range where they are generally positively correlated with CO_2 production in lakes,[46] and MeHg concentrations in water and organisms (Figure 4).[47, 48] At DOC concentrations higher than 10 mg/L, a negative relationship with MeHg concentrations in water and organisms has sometimes been observed, in part related to the lower Hg bioavailability if bound to DOC.[47-49] The bacterial respiration has also been shown to respectively plateau or decline at the highest DOC and TP ranges from several lakes (>10 mg/L and >11 µg/L, respectively).[46] We suggest to include more often the measurement of CO_2 concentrations in future Hg studies to better explain the DOC vs. MeHg relationships.[50]

Hg concentrations in soils, water, and sediments are strongly correlated with the amount of organic matter in these matrices.[51, 52] Here, bacterial decomposition of allochthonous and autochthonous organic carbon having a $\delta^{13}C$ of −28‰[53] led to the production of ^{13}C-depleted CO_2 of a similar $\delta^{13}C$ signature.[44, 45] Atmospheric CO_2 had a $\delta^{13}C$ value of −10.4‰ ± 0.5‰ (± SD, *n* = 9, Figure 4a). The $\delta^{13}C$-CO_2 values in water ranged from −15‰ to −23‰ (Figure 4), indicating that approximately one to two third of the dissolved CO_2 originated from heterotrophically respired CO_2.[44, 54] Carbon dioxide used by primary producers during photosynthesis further fractionated the carbon isotopes (fractionation of approx. −16‰ for lotic benthic algae having a small boundary layer)[55] to lead to biogenic $\delta^{13}C$ values of −31 to −39‰. We recorded organismal $\delta^{13}C$ values in this range (Figure 3), although we observed even more depleted values as well (Figure 3b), suggesting a more important contribution of heterotrophically respired CO_2 in some sectors,

or a contribution of oxidized methane having a $\delta^{13}C$ of −42 ± 8‰ (n = 17; ± SD). Run-of-river pondages CAUP and RDC have been influenced by organic matter inputs subsequent to wildfire and logging activities; thus, organic matter degradation and concurrent Hg methylation (Figure 4d),[10] as well as the release of nutrients (Figure 4c), likely favored primary production, MeHg algal uptake, and its transfer up the food chain. Considering that DOC, TP, %MeHg, and CO_2 were higher in CAUP, in contrast to RDC (Figure 4), we suggest that the wildfire in the CAUP watershed led to a short-term rise in MeHg favored by autochthonous productivity (as in the sector CC; Figure 4). In contrast, the RDC watershed influenced by logging could have released allochthonous DOC and probably, terrestrially-produced MeHg over a longer period, leading to a longer fish contamination in that sector (Figure 2).[56] In rivers impacted by run-of-river pondages, flooded bays and plains are sites of terrestrial organic matter accumulation and recycling, Hg methylation, and high production.[43] Our study revealed that $\delta^{13}C$ could track both Hg methylation and organic carbon processing as well as bolster predictions of MeHg accumulation within aquatic food webs.

Trophic Magnification Slope among Sectors. Highly significant ($p < 0.0001$) relationships were obtained between the entire food web [MeHg] and the $\delta^{15}N_{adj}$ of specific sectors in 2016 (Figure S6a and S7; statistical details in Table S4). Overall, the whole food web TMS values did not show any upstream–downstream trends. The lowest TMS was measured in the constructed wetlands (CC), and similar values were calculated for the adjacent pondage CAUP and sector MR ($p > 0.05$). The TMS from the RDC pondage food web was significantly higher than that from CAUP and CC. In our most downstream sector, the Blanc Reservoir (BR), TMS was similar to the upstream site NSM. TMSs calculated for high trophic level fish (Figure S6b) were generally greater than those of

the whole food web (Figure S6a).[57] There was no significant difference between TMSs among sectors for high trophic level fish. Overall, TMS values varied greatly, and one of the lowest TMS was measured in the most Hg-contaminated sector (CAUP). We therefore deepened our analysis to investigate what possible factors influenced TMS values.

Influence of Chemistry and Low Trophic Level Processes on Biomagnification. TMSs calculated using all organisms (Figure S6a) produced a wide range of values comparable to those obtained from a worldwide meta-analysis.[18] TMSs were positively correlated with the average organismal $\delta^{13}C$ (Figure 5a). This likely indicates that decomposition of organic matter from allochthonous and autochthonous origins and the associated release (Figure 4a) and uptake of ^{13}C-depleted CO_2 was associated with MeHg accumulation at low trophic levels (Figure 3) and the change in TMSs (Figure 5d). There is a mathematical dependency in Figure 5d but according to Verburg,[58] the more plausible mathematical condition that could have influenced TMS values was the higher [MeHg] variation among sectors for low trophic levels compared to high trophic levels.[58] TMSs were also negatively correlated with nutrients (Figure 5b) and the proportion of MeHg in water (Figure 5c). These correlations are probably an indirect effect of higher MeHg accumulation within low trophic levels in conditions where there are higher concentrations of nutrients and MeHg in water (Figure S8b–d). Our results are consistent with those of Clayden et al.[19], who reported low TMSs in lakes characterized by high concentrations of dissolved MeHg and nutrients. These interdependent environmental parameters indirectly affected TMS through the change in MeHg concentrations at low trophic levels (Figure 5d). These findings must be considered in future studies when interpreting TMSs for tracking MeHg biomagnification.

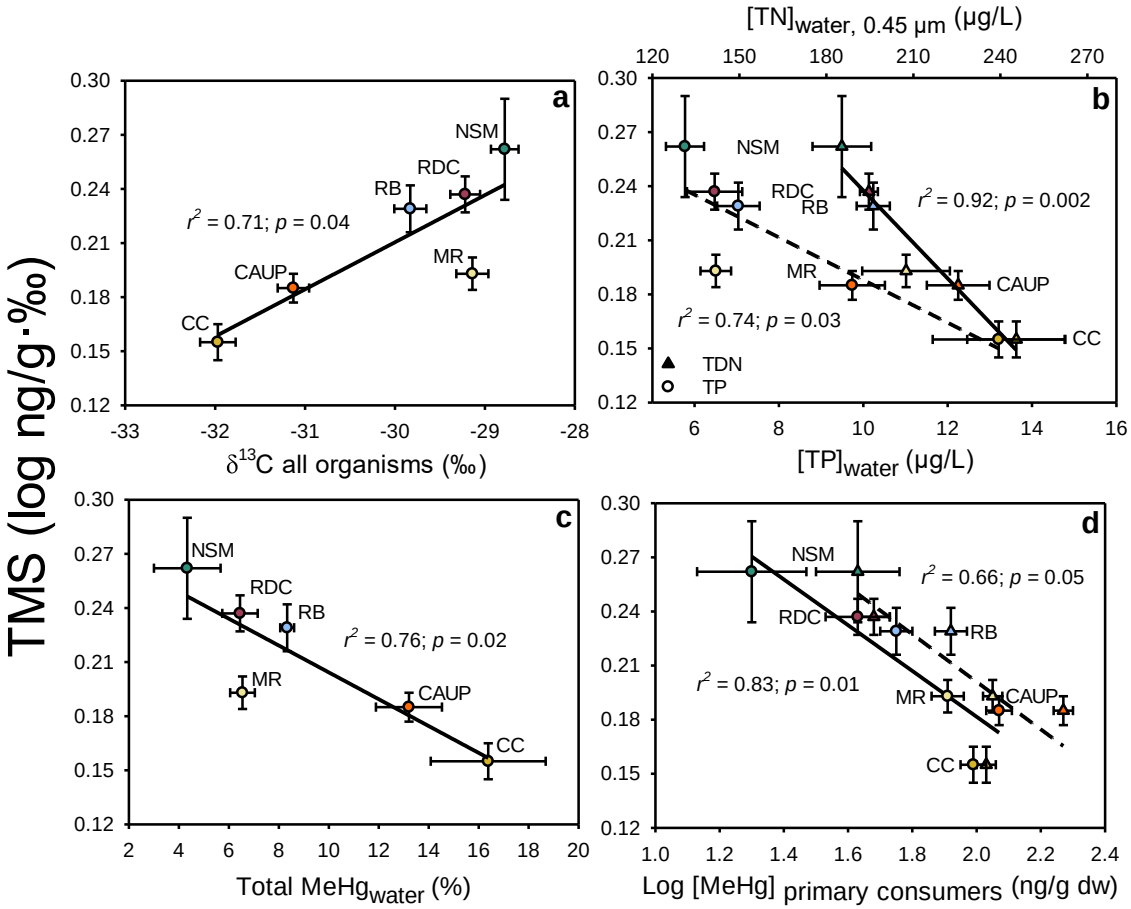

438

439 **Figure 5.** Trophic magnification slopes (TMS, log ng/g·‰ ± SE, from Figure 6a) as a function of (a)
440 organismal $\delta^{13}C$ from all organisms sampled within a specific sector; (b) total dissolved nitrogen
441 ($[TN]_{water,\ 0.45\ \mu m}$, µg/L ± SE, n = 3–48) and aqueous total phosphorous ($[TP]_{water}$, µg/L ± SE, n = 3–
442 48); (c) aqueous proportions of total MeHg (total [MeHg]/total [Hg] × 100, % ± SE, n = 3–48); and
443 (d) primary consumer [MeHg] (circles and solid line, log[MeHg] ± SE, Table S2) and trophic
444 magnification intercepts (TMI, triangles and dashed line, log[MeHg], ng/g dw ± SE, Table S2).
445 Sectors are indicated with their abbreviation.

446

447 **Carbon Isotopes to Better Predict MeHg Bioaccumulation.** The overall (all sectors combined)
448 relationship of [MeHg] as a function of $\delta^{15}N_{adj}$ predicted 67% of [MeHg] variability in invertebrates
449 and fish (Figure 6a). Both $\delta^{15}N_{adj}$ and $\delta^{13}C$ explained part of the variability of MeHg
450 bioaccumulation in fish and invertebrates (Figures 3 and S6). Some of this variability was also
451 explained by differences between sectors as suggested by the significant differences between

TMSs (Figure S7). We ran a linear mixed model (LMM) that accounted for $\delta^{13}C$, $\delta^{15}N_{adj}$, and sector influences. This model explained 80% (conditional $r^2 = 0.80$) of the variability in food web [MeHg]. Nine percent (marginal $r^2 = 0.71$) of this overall variation related to intersector differences. Figure 6b presents the model with the sector differences removed. When relying on both isotopic signatures, we predicted 71% (Figure 6b) of the MeHg concentrations, whereas 67% of the variability was explained when using only $\delta^{15}N_{adj}$ (Figure 6a). The slope of the regression in Figure 6b is closer to one, and the intercept is closer to zero, indicating a better prediction for the LMM (AIC = 322) than the simple regression model from Figure 6a (AIC = 445, ANCOVA: $p = 0.002$). Furthermore, we performed independent LMM comparisons ($\delta^{15}N_{adj}$, $\delta^{13}C$, and $\delta^{15}N_{adj} + \delta^{13}C$) for primary and secondary consumer invertebrates, low and high trophic level fish, and by grouping all invertebrates and all fish (Table S3). In all cases, the model using both isotopic signatures was more accurate than using only $\delta^{15}N_{adj}$ (Table S3; AIC >4). For primary consumers and low trophic level fish, the combined model ($\delta^{15}N_{adj} + \delta^{13}C$) was not better than using $\delta^{13}C$ alone (Table S3), further indicating the relevance of considering carbon processing ($\delta^{13}C$) along with trophodynamics ($\delta^{15}N_{adj}$) in MeHg bioaccumulation prediction models.

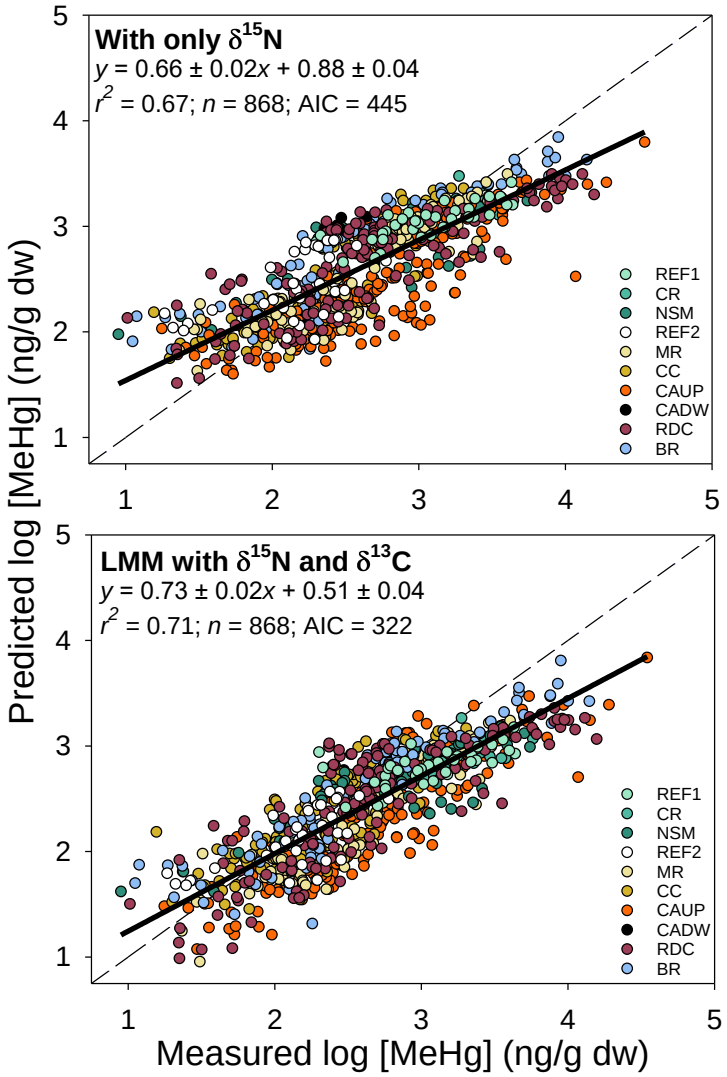

Figure 6. Predicted log [MeHg] (ng/g dw) as a function of measured log [MeHg] (ng/g dw) for all sampled organisms and all sectors together. (a) Simple regression model with $\delta^{15}N$ (‰). (b) A linear mixed model including the carbon stable isotope ($\delta^{13}C$, ‰) and nitrogen stable isotope ($\delta^{15}N$, ‰) signatures. The slopes for both fixed variables $\delta^{15}N$ and $\delta^{13}C$ are 0.21 ± 0.01 and −0.06 ± 0.02 ($p < 0.001$), respectively. For the linear mixed model (LMM), if sectors are set as a random effect, $r^2 = 0.80$. The two models (a and b) are significantly different ($p = 0.002$).

Relationships between [MeHg] and $\delta^{13}C$ have been observed for lake organisms,[59, 60] with pelagic organisms having higher [MeHg] and lower $\delta^{13}C$ compared to littoral organisms.[22, 61-63] Few studies have related organism [MeHg] to $\delta^{13}C$ in streams or rivers. One reason is that the $\delta^{13}C$ range is generally larger in lakes than in rivers because of the higher methanogenesis and CO_2

recycling in lakes, and related methylation.[44, 50, 64] We found only one study in lotic environments that observed $\delta^{13}C$ to be a better predictor than $\delta^{15}N$ for determining Hg accumulation in stream macroinvertebrates.[65] The authors linked this observation to, at least in part, scrapers and filterers foraging in sun-exposed sites characterized by a higher production of periphytic biofilm (low $\delta^{13}C$ and high Hg) as compared with invertebrates in shaded sites that forage on land detritus (high $\delta^{13}C$ and low Hg). We suggest that a similar process is occurring at various extents for periphyton-based vs. detrital-based food chains, pelagic vs. littoral organisms, or in the present case, between run-of-river pondages vs. upstream site organisms. The former locations (periphyton-based food chain, pelagic zones and pondages) are where degradation of organic matter (leading to low $\delta^{13}C$ values) and parallel MeHg formation occur predominantly. Furthermore, the nutrients associated with the terrestrial organic matter inputs lead to greater algal production and MeHg trophic transfer. We propose that the rather slow degradation of Hg-rich allochthonous organic matter in flooded plains and bays from run-of-river pondages fuels the primary production by the release of nutrients, and thus favor the presence of autochthonous material more prone to bacterial degradation and parallel Hg methylation.[56] Those nutrient-rich environments are ideal for foraging and MeHg trophic transfer.

Run-of-river impoundments accumulate organic matter transported from upstream sources released through landscape disturbances, e.g. logging and forest fires, fueling nutrient release, Hg methylation, biological production, and MeHg food web transfer. Additional studies should assess whether these Hg surges are common, particularly in landscapes modified by multiple natural and anthropogenic disturbances.

ACKNOWLEDGMENTS

This research was funded by a collaborative research and development (CRD) grant to MA and DP from the Natural Sciences and Engineering Research Council of Canada (NSERC) and Hydro-Québec. DEP and RAL received postdoctoral NSERC CREATE fellowships, and ML received a FRQNT scholarship. MA thanks the Canada Research Chair program.

ASSOCIATED CONTENT

The Supporting Information is available free of charge on the ACS publications website. This file includes 6 text sections, 4 tables, and 8 figures.

LITERATURE CITED

1. Grill, G.; Lehner, B.; Lumsdon, A. E.; MacDonald, G. K.; Zarfl, C.; Liermann, C. R., An index-based framework for assessing patterns and trends in river fragmentation and flow regulation by global dams at multiple scales. *Environ. Res. Lett.* **2015,** *10*, (1), 015001.

2. Zarfl, C.; Lumsdon, A. E.; Berlekamp, J.; Tydecks, L.; Tockner, K., A global boom in hydropower dam construction. *Aquat. Sci.* **2015,** *77*, (1), 161-170.

3. Couto, T. B. A.; Olden, J. D., Global proliferation of small hydropower plants - science and policy. *Front. Ecol. Environ.* **2018,** *16*, (2), 91-100.

4. Maavara, T.; Lauerwald, R.; Regnier, P.; Van Cappellen, P., Global perturbation of organic carbon cycling by river damming. *Nat. Comm.* **2017,** *8*, 15347.

5. Vorosmarty, C. J.; Meybeck, M.; Fekete, B.; Sharma, K.; Green, P.; Syvitski, J. P. M., Anthropogenic sediment retention: major global impact from registered river impoundments. *Global Planet. Change* **2003,** *39*, (1-2), 169-190.

6. Health-Canada, Human Health Risk Assessment of Mercury in Fish and Health Benefits of Fish Consumption. In Branch, B. o. C. S. F. D. H. P. a. F., Ed. Health Canada: Ottawa, 2007; p 76.

7. Bilodeau, F.; Therrien, J.; Schetagne, R., Intensity and duration of effects of impoundment on mercury levels in fishes of hydroelectric reservoirs in northern Quebec (Canada). *Inland Waters* **2017,** *7*, (4), 493-503.

8. Anderson, D.; Moggridge, H.; Warren, P.; Shucksmith, J., The impacts of "run-of-river' hydropower on the physical and ecological condition of rivers. *Water Environ. J.* **2015,** *29*, (2), 268-276.

9. Silverthorn, V. M.; Bishop, C. A.; Jardine, T.; Elliott, J. E.; Morrissey, C. A., Impact of flow diversion by run-of-river dams on american dipper diet and mercury exposure. *Environ. Toxicol. Chem.* **2018,** *37*, (2), 411-426.

10. Paranjape, A. R.; Hall, B. D., Recent advances in the study of mercury methylation in aquatic systems. *Facets* **2017,** *2*, 85-119.

11. Kelly, C. A.; Rudd, J. W. M.; Bodaly, R. A.; Roulet, N. P.; StLouis, V. L.; Heyes, A.; Moore, T. R.; Schiff, S.; Aravena, R.; Scott, K. J.; Dyck, B.; Harris, R.; Warner, B.; Edwards, G., Increases in fluxes of greenhouse gases and methyl mercury following flooding of an experimental reservoir. *Environ. Sci. Technol.* **1997,** *31*, (5), 1334-1344.

12. Barros, N.; Cole, J. J.; Tranvik, L. J.; Prairie, Y. T.; Bastviken, D.; Huszar, V. L. M.; del Giorgio, P.; Roland, F., Carbon emission from hydroelectric reservoirs linked to reservoir age and latitude. *Nat. Geosci.* **2011,** *4*, (9), 593-596.

13. Schetagne, R., Water quality modifications after impoundment of some large northern reservoirs. *Ergebnisse der Limnologie* **1994,** *40*, 223-229.

14. Peterson, B. J.; Fry, B., Stable isotopes in ecosystem studies. *Ann. Rev. Ecol. Syst.* **1987,** *18*, 293-320.

15. Bonzongo, J. C. J.; Donkor, A. K.; Attibayeba, A.; Gao, J., Linking landscape development intensity within watersheds to methyl-mercury accumulation in river sediments. *Ambio* **2016,** *45*, (2), 196-204.

16. Garcia, E.; Carignan, R., Mercury concentrations in northern pike (*Esox lucius*) from boreal lakes with logged, burned, or undisturbed catchments. *Can. J. Fish. Aquat. Sci.* **2000,** *57*, 129-135.

17. Dang, F.; Wang, W. X., Why mercury concentration increases with fish size? Biokinetic explanation. *Environ. Poll.* **2012,** *163*, 192-198.

18. Lavoie, R. A.; Jardine, T. D.; Chumchal, M. M.; Kidd, K. A.; Campbell, L. M., Biomagnification of mercury in aquatic food webs: A worldwide meta-analysis. *Environ. Sci. Technol.* **2013,** *47*, (23), 13385-13394.

19. Clayden, M. G.; Kidd, K. A.; Wyn, B.; Kirk, J. L.; Muir, D. C. G.; O'Driscoll, N. J., Mercury biomagnification through food webs is affected by physical and chemical characteristics of lakes. *Environ. Sci. Technol.* **2013,** *47*, (21), 12047-12053.

20. Baumgartner, M. T.; Piana, P. A.; Baumgartner, G.; Gomes, L. C., Storage or run-of-river reservoirs: exploring the ecological effects of dam operation on stability and species interactions of fish assemblages. *Environ. Manage.* **2020,** *65*, (2), 220-231.

21. Bilotta, G. S.; Burnside, N. G.; Turley, M. D.; Gray, J. C.; Orr, H. G., The effects of run-of-river hydroelectric power schemes on invertebrate community composition in temperate streams and rivers. *PLoS One* **2017,** *12*, (2), 13.

22. Stewart, A. R.; Saiki, M. K.; Kuwabara, J. S.; Alpers, C. N.; Marvin-DiPasquale, M.; Krabbenhoft, D. P., Influence of plankton mercury dynamics and trophic pathways on mercury concentrations of top predator fish of a mining-impacted reservoir. *Can. J. Fish. Aquat. Sci.* **2008,** *65*, (11), 2351-2366.

23. Houde, L., Teneurs en mercure dans les poissons du réservoir Gouin en 2002. In Bibliothèque National du Québec: Montreal, Quebec, Canada, 2004; p 21.

24. AECOM, Aménagements hydroélectriques de la Chute-Allard et des Rapides-des-Coeurs. Suivis des communautés de poissons dans les biefs de la Chute-Allard et des Rapides des

578 Coeurs. Suivi environnemental 2013 en phase d'exploitation. In Hydro-Québec Production:
579 Direction Production des Cascades, 2014; p 58.

580 25. AECOM, Aménagements hydroélectriques de la Chute-Allard et des Rapides-des-Coeurs.
581 Suivis des communautés de poissons dans les biefs de la Chute-Allard et des Rapides des
582 Coeurs. Suivi environnemental 2016 en phase d'exploitation. In Hydro-Québec Production:
583 Direction Production des Cascades, 2017; p 115.

584 26. AECOM, Aménagements hydroélectriques de la Chute-Allard et des Rapides-des-Coeurs.
585 Teneurs en mercure dans la chair des poissons. Suivi environnemental 2013 en phase
586 d'exploitation. In Hydro-Québec Production: 2014; p 59.

587 27. Sacotte, S.; Bilodeau, F., Aménagements hydroélectriques de la Chute-Allard et des
588 Rapides-des-Coeurs. Teneurs en mercure dans la chair des poissons. Suivi environnemental
589 2016 en phase d'exploitation. In Hydro-Québec Production: 2017; p 87.

590 28. Desroches, J. F.; Picard, I., *Poissons d'eau douce du Québec et des Maritimes*. 2013; p
591 472.

592 29. Hintelmann, H.; Nguyen, H., Extraction of methylmercury from tissue and plant samples
593 by acid leaching. *Anal. Bioanal. Chem.* **2005,** *381*, (2), 360-365.

594 30. Khadra, M.; Caron, A.; Planas, D.; Ponton, D. E.; Rosabal, M.; Amyot, M., The fish or the
595 egg: Maternal transfer and subcellular partitioning of mercury and selenium in Yellow Perch
596 (*Perca flavescens*). *Sci. Tot. Environ.* **2019,** *675*, 604-614.

31. Tremblay, G.; Legendre, P.; Doyon, J. F.; Verdon, R.; Schetagne, R., The use of polynomial regression analysis with indicator variables for interpretation of mercury in fish data. *Biogeochemistry* **1998,** *40*, (2-3), 189-201.

32. Post, D. M., Using stable isotopes to estimate trophic position: Models, methods, and assumptions. *Ecology* **2002,** *83*, (3), 703-718.

33. Burnham, K. P.; Anderson, D. R.; Huyvaert, K. P., AIC model selection and multimodel inference in behavioral ecology: some background, observations, and comparisons. *Behav. Ecol. Sociobiol.* **2011,** *65*, (1), 23-35.

34. Cebalho, E. C.; Diez, S.; Filho, M. D.; Muniz, C. C.; Lazaro, W.; Malm, O.; Ignacio, A. R. A., Effects of small hydropower plants on mercury concentrations in fish. *Environ. Sci. Poll. Res.* **2017,** *24*, (28), 22709-22716.

35. Bozek, M. A.; Haxton, T. J.; Raabe, J. K., *Walleye and Sauger Habitat*. American Fisheries Society: 2011; p 570.

36. Bae, H. S.; Dierberg, F. E.; Ogram, A., Periphyton and Flocculent Materials Are Important Ecological Compartments Supporting Abundant and Diverse Mercury Methylator Assemblages in the Florida Everglades. *Appl. Environ. Microbiol.* **2019,** *85*, (13, e00156-19), 1-17.

37. Herendeen, R. A.; Hill, W. R., Growth dilution in multilevel food chains. *Ecol. Model.* **2004,** *178*, (3-4), 349-356.

38. Wang, W. X., Biodynamic understanding of mercury accumulation in marine and freshwater fish. *Adv. Environ. Res.* **2012,** *1*, (1), 15-35.

39. Garcia, E.; Carignan, R., Impact of wildfire and clear-cutting in the boreal forest on methyl mercury in zooplankton. *Can. J. Fish. Aquat. Sci.* **1999,** *56*, (2), 339-345.

40. Porvari, P.; Verta, M.; Munthe, J.; Haapanen, M., Forestry practices increase mercury and methyl mercury output from boreal forest catchments. *Environ. Sci. Technol.* **2003,** *37*, (11), 2389-2393.

41. Willacker, J. J.; Eagles-Smith, C. A.; Kowalski, B. M.; Danehy, R. J.; Jackson, A. K.; Adams, E. M.; Evers, D. C.; Eckley, C. S.; Tate, M. T.; Krabbenhoft, D. P., Timber harvest alters mercury bioaccumulation and food web structure in headwater streams. *Environ. Poll.* **2019,** *253*, 636-645.

42. Garcia, E.; Carignan, R., Mercury concentrations in fish from forest harvesting and fire-impacted Canadian boreal lakes compared using stable isotopes of nitrogen. *Environ. Toxicol. Chem.* **2005,** *24*, (3), 685-693.

43. Millera Ferriz, L.; Storck, V.; Ponton, D. E.; Leclerc, M.; Bilodeau, F.; Walsh, D.; Amyot, M., Methylmercury and methylating microbial community profiles in river sediments affected by run-of-the-river hydroelectric power plants. *Sci. Tot. Environ.* **accepted**.

44. Lennon, J. T.; Faiia, A. M.; Feng, X. H.; Cottingham, K. L., Relative importance of CO_2 recycling and CH_4 pathways in lake food webs along a dissolved organic carbon gradient. *Limnol. Oceanogr.* **2006,** *51*, (4), 1602-1613.

635 45. Smyntek, P. M.; Maberly, S. C.; Grey, J., Dissolved carbon dioxide concentration controls
636 baseline stable carbon isotope signatures of a lake food web. *Limnol. Oceanogr.* **2012,** *57*, (5),
637 1292-1302.

638 46. Lapierre, J. F.; del Giorgio, P. A., Geographical and environmental drivers of regional
639 differences in the lake pCO(2) versus DOC relationship across northern landscapes. *J. Geophys.*
640 *Res. Biogeosci.* **2012,** *117*.

641 47. Driscoll, C. T.; Yan, C.; Schofield, C. L.; Munson, R.; Holsapple, J., The mercury cycle and
642 fish in the Adirondack lakes. *Environ. Sci. Technol.* **1994,** *28*, (3), A136-A143.

643 48. Broadley, H. J.; Cottingham, K. L.; Baer, N. A.; Weathers, K. C.; Ewing, H. A.; Chaves-Ulloa,
644 R.; Chickering, J.; Wilson, A. M.; Shrestha, J.; Chen, C. Y., Factors affecting MeHg
645 bioaccumulation in stream biota: the role of dissolved organic carbon and diet. *Ecotoxicology*
646 **2019,** *28*, (8), 949-963.

647 49. Schartup, A. T.; Qureshi, A.; Dassuncao, C.; Thackray, C. P.; Harding, G.; Sunderland, E.
648 M., A Model for Methylmercury Uptake and Trophic Transfer by Marine Plankton. *Environ. Sci.*
649 *Technol.* **2018,** *52*, (2), 654-662.

650 50. De Bonville, J.; Amyot, M.; del Giorgio, P.; Tremblay, A.; Bilodeau, F.; Ponton, D. E.;
651 Lapierre, J. F., Mobilization and transformation of mercury across a dammed boreal river are
652 linked to carbon processing and hydrology. *Water Resour. Res.* **2020,** *56*, (10), e2020WR027951.

51. Schartup, A. T.; Mason, R. P.; Balcom, P. H.; Hollweg, T. A.; Chen, C. Y., Methylmercury production in estuarine sediments: role of organic matter. *Environ. Sci. Technol.* **2013,** *47*, (2), 695-700.

52. Lavoie, R. A.; Amyot, M.; Lapierre, J. F., Global meta-analysis on the relationship between mercury and dissolved organic carbon in freshwater environments. *J. Geophys. Res. Biogeosci.* **2019,** *124*, (6), 1508-1523.

53. Finlay, J. C., Stable-carbon-isotope ratios of river biota: Implications for energy flow in lotic food webs. *Ecology* **2001,** *82*, (4), 1052-1064.

54. Phillips, D. L.; Gregg, J. W., Uncertainty in source partitioning using stable isotopes. *Oecologia* **2001,** *127*, (2), 171-179.

55. Hecky, R. E.; Hesslein, R. H., Contributions of benthic algae to lake food webs as revealed by stable isotope analysis. *J. N. Am. Benthol. Soc.* **1995,** *14*, (4), 631-653.

56. Bravo, A. G.; Bouchet, S.; Tolu, J.; Bjorn, E.; Mateos-Rivera, A.; Bertilsson, S., Molecular composition of organic matter controls methylmercury formation in boreal lakes. *Nat. Comm.* **2017,** *8*.

57. Jennings, S.; van der Molen, J., Trophic levels of marine consumers from nitrogen stable isotope analysis: estimation and uncertainty. *ICES J. Mar. Sci.* **2015,** *72*, (8), 2289-2300.

58. Verburg, P., Lack of evidence for lower mercury biomagnification by biomass dilution in more productive lakes: Comment on "Mercury biomagnification through food webs is affected

672 by physical and chemical characteristics of lakes". *Environ. Sci. Technol.* **2014,** *48*, (17), 10524-
673 10525.

674 59. Montgomery, S.; Lucotte, M.; Cournoyer, L., The use of stable carbon isotopes to
675 evaluate the importance of fine suspended particulate matter in the transfer of methylmercury
676 to biota in boreal flooded environments. *Sci. Tot. Environ.* **2000,** *261*, (1-3), 33-41.

677 60. Power, M.; Klein, G. M.; Guiguer, K.; Kwan, M. K. H., Mercury accumulation in the fish
678 community of a sub-Arctic lake in relation to trophic position and carbon sources. *J. Appli. Ecol.*
679 **2002,** *39*, (5), 819-830.

680 61. Chetelat, J.; Amyot, M.; Garcia, E., Habitat-specific bioaccumulation of methylmercury in
681 invertebrates of small mid-latitude lakes in North America. *Environ. Poll.* **2011,** *159*, (1), 10-17.

682 62. Tremblay, A.; Lucotte, M., Accumulation of total mercury and methyl mercury in insect
683 larvae of hydroelectric reservoirs. *Can. J. Fish. Aquat. Sci.* **1997,** *54*, (4), 832-841.

684 63. Tremblay, A.; Lucotte, M.; Schetagne, R., Total mercury and methylmercury
685 accumulation in zooplankton of hydroelectric reservoirs in northern Quebec (Canada). *Sci. Tot.*
686 *Environ.* **1998,** *213*, (1-3), 307-315.

687 64. Jones, R. I.; Carter, C. E.; Kelly, A.; Ward, S.; Kelly, D. J.; Grey, J., Widespread contribution
688 of methane-cycle bacteria to the diets of lake profundal chironomid larvae. *Ecology* **2008,** *89*,
689 (3), 857-864.

690 65. Riva-Murray, K.; Bradley, P. M.; Chasar, L. C.; Button, D. T.; Brigham, M. E.; Eikenberry, B.
691 C. S.; Journey, C. A.; Lutz, M. A., Influence of dietary carbon on mercury bioaccumulation in
692 streams of the Adirondack Mountains of New York and the Coastal Plain of South Carolina, USA.
693 *Ecotoxicology* **2013,** *22*, (1), 60-71.

694